Scalar Transport Characteristics of the Linear-Eddy Model

S. M. DEBRUYNKOPS* and J. J. RILEY

Department of Mechanical Engineering, University of Washington, Box 352600, Seattle, WA 98195-2600

The properties of the linear-eddy model (LEM) are investigated by applying it to the problem of plume dispersion from a line source in homogeneous turbulence. It is concluded that the LEM performs better than previously reported if the decay of the turbulence is taken into account. Also noted is an apparently unphysical characteristic of the LEM that results in a single realization of the stochastic model yielding results, at late times, equivalent to a temporal average.

BACKGROUND

The linear-eddy model (LEM) for turbulent transport has been applied to several different flows and correctly predicts various characteristics of turbulent mixing. These include key features of scalar power spectra for a mixing layer in grid turbulence [1] and many aspects of mixing in a jet such as differential diffusion effects [2]. Implementation of the LEM as a subgrid model in large-eddy simulations of reacting flows has also been shown to realistically represent important features of the turbulent mixing process [3, 4]. In order to further evaluate its potential, we have made additional comparisons of model results with laboratory experiments.

In the LEM, the time development of a passive scalar field in turbulence is modeled as the superposition of two processes, (1) molecular diffusion and (2) convective stirring, both applied on a one-dimensional domain. Molecular diffusion is treated directly through the solution of the diffusion equation assuming Fick's law. Convective stirring is implemented as a stochastic process consisting of inversion events. Each event is a map of a segment of the field onto itself; the frequency, size, and mapping functions of the events are related to the properties of the turbulent flow field. The time development of the scalar field is numerically computed for individual realizations, and statistics of the field are computed from an ensemble average, usually of 1000 or more realizations.

The problem we address is a plume downstream of a line source in homogeneous turbulence, which has been the subject of significant theoretical and experimental research (see, e.g., [5]–[10]). The axis of the line source is taken as the z axis, and is perpendicular to the direction of the mean flow, taken as the x direction. When viewed in a fixed laboratory reference frame, the problem is statistically stationary and two dimensional, with statistical quantities depending on the streamwise coordinate x and the transverse (to the line source) coordinate y. In order to model this with the LEM, it is convenient to consider the flow in a reference frame moving with the mean flow. Then, invoking Taylor's hypothesis, the statistical quantities depend on y and time t ($= x/\overline{u}$), where $\overline{u}$ is the mean velocity.

The corresponding LEM is defined with a point source at $y = 0$, and the profile of the scalar for a single realization of the model is denoted $\theta(y,t)$. The initial and boundary conditions are $\theta(y,0) = \delta(y)$, where $\delta(y)$ is the Dirac delta function and $\theta(\pm\infty,t) = 0$. The general behavior described in this paper is independent of the model formulation, but, for specificity, the following characteristics are used (see [1] for analytic development): the probability density of an eddy of size s is $f(s) = \delta(s - L)$, where L is the integral length scale of the velocity field, i.e., a single eddy size is assumed; the frequency of eddy events is $(54/4)D_T/L^3$, where D_T is the turbulent diffusivity as defined by Tennekes and Lumley

* Corresponding author.

COMBUSTION AND FLAME 112: 253–260 (1998)

Published by Elsevier Science Inc.

0010-2180/98/$19.00
PII S0010-2180(97)00116-8

[11, p. 11]; the mapping function from $\theta(y)$ before an inversion event to $\theta^*(y)$ after an inversion is

$$\theta^*(y) = \begin{cases} \theta(3y - 2y_0), \\ \quad \text{if } y_0 \le y \le y_0 + \frac{1}{3}s. \\ \theta(-3y + 4y_0 + 2s), \\ \quad \text{fi } y_0 + \frac{1}{3}s \le y \le y_0 + \frac{2}{3}s. \\ \theta(3y - 2y_0 - 2s), \\ \quad \text{if } y_0 + \frac{2}{3}s \le y \le y_0 + s. \\ \theta, \quad \text{otherwise.} \end{cases}$$

where y_0 is the coordinate of the center of the inversion. With this mapping, a section of the discrete numeric field having the values 1-2-3-4-5-6 before the inversion has values 1-4-5-2-3-6 after the inversion.

EXPECTED BEHAVIOR

Laboratory experiments support the conclusion made by Gifford [6] and Corrsin [7] that the plume undergoes two simultaneous processes. In one, small-scale turbulence and molecular diffusion disperse the scalar to produce a wider plume. At the same time, larger eddies advect it from side to side. Many aspects of the predictions by the LEM of the plume's behavior are available in the literature [12], but of special interest here is the large-scale, side-to-side motion which we will refer to as flapping. Two measurements of this characteristic are the motion of the plume center and the centerline value of the root mean square (rms) fluctuation normalized by the mean value, i.e., $(\theta'/\bar{\theta})_{CL}$.

To make estimates of the behavior of these quantities, consider a laboratory experiment involving a thin plume which does not spread very rapidly compared with the rate at which it flaps in the transverse direction; then Chandrasekhar's analysis of the random walk of a marker particle [13] provides an estimate of the evolution of the location of the plume center. Based on this model, the location of the plume center will have a Gaussian probability density function, the variance σ^2 of which is $\sigma^2 = 2D_T t$. For turbulent flows, D_T is proportional to $u'L$, where u' is the rms of the turbulent velocity fluctuations [11]. Thus D_T is constant in both the case of nondecaying turbulence and also in the case where the turbulence decays with $u' \sim t^{-1/2}$ and $L \sim t^{1/2}$. When D_T is constant, then $\sigma^2 \sim t$. Clearly the plume will wander away from the centerline.

This reasoning leads to the conclusion that $(\theta'/\bar{\theta})_{CL}$ will not be zero, since a zero value implies that the scalar concentration on the centerline at a given downstream location is constant in time, which is inconsistent with the concept that the plume flaps. Based on his experimental data, Warhaft indicates that the ratio tends to a constant value of about 0.7 [10]. Since a constant value for the ratio is consistent with a self-similar solution, it is informative to determine under what conditions such a self-similar solution can exist. Let $u(t)$ be the characteristic scale of the velocity fluctuations, $l(t)$ be the length scale of $\bar{\theta}$, $\theta_0(t)$ be the scale of the scalar fluctuations, and define the similarity variable $\xi = y/l(t)$. Then assume self-similar forms,

$$\bar{\theta}(t, y) = \theta_0 F(\xi), \tag{1}$$

$$\overline{\theta' v'}(t, y) = \theta_0 u G(\xi), \tag{2}$$

$$\overline{\theta'^2 v'}(t, y) = \theta_0^2 u H(\xi), \tag{3}$$

$$\overline{\theta'^2}(t, y) = \theta_0^2 J(\xi), \tag{4}$$

where F, G, H, J are unknown functions and v' is the velocity fluctuation in the y direction. By assuming homogeneity in z and that $\partial(\,)/\partial x \ll \partial(\,)/\partial y$, and using Taylor's hypothesis to replace $\underline{x/\bar{u}}$ with t, the transport equations for $\bar{\theta}$ and θ'^2 become

$$\frac{\partial \bar{\theta}}{\partial t} = -\frac{\partial \overline{\theta' v'}}{\partial y} + D_M \frac{\partial^2 \bar{\theta}}{\partial y^2}, \tag{5}$$

$$\frac{1}{2}\frac{\partial \overline{\theta'^2}}{\partial t} = -\overline{\theta' v'}\frac{\partial \overline{\theta'^2}}{\partial y} - \frac{1}{2}\frac{\partial \overline{\theta'^2 v'}}{\partial y}, \tag{6}$$

where D_M is the molecular diffusivity of the scalar. Substituting Eqs. 1–4 into Eqs. 5 and 6

indicates that the following expressions must be constant for a similarity solution to exist:

$$\frac{l}{u\theta_0}\frac{d\theta_0}{dt}, \quad \frac{1}{u}\frac{dl}{dt}, \quad \frac{1}{ul}.$$

In addition, noting from Eq. 5 that the lateral integral of $\bar{\sigma}$ is constant at all times, then $\theta_0 l$ must also be constant. Hence, if $u \propto t^{-1/2}$, then $l \propto t^{1/2}$ and $\theta_0 \propto t^{-1/2}$, and it is possible for the plume to be self-similar. Self-similar behavior is not expected for cases where $u \propto t^{-n}$ and $n \neq 1/2$. In particular this applies to nondecaying turbulence ($n = 0$). Tennekes and Lumley present a similar argument [11, Chap. 7].

RESULTS

We used the LEM to simulate the behavior of a thermal plume downstream of a heated wire placed on the centerline ($y = 0$) in a homogeneous turbulence field. The parameters for the four cases examined are given in Table 1. They are intended to model the flow field studied by Warhaft [10], with case A statistically stationary, case B decaying at the rate predicted by several theories for high Reynolds numbers [11], and case C decaying at the rate observed by Warhaft. In case D, L grows faster than $t^{1/2}$ and the Reynolds number is constant.

Implementation of the turbulent decay scheme relies on scaling laws for D_T and t_L, i.e., $D_T \propto L^2/t_L$ and $t_L \propto L/u'$. Following Kerstein [12], the constants of proportionality in these expressions are taken to be unity. At each time step, L and u' are determined in terms of their initial values and the simulated time, and D_T is updated. Then the frequency of eddy events, λ, is computed as $\lambda = (54/4)D_T/L^3$. Hence, all the model parameters affected by the turbulence decay are adjusted at each time step. The remaining parameter (molecular diffusivity) is held constant throughout the simulation.

TABLE 1

Simulation Parameters[a]

Case	Initial Re_L	Sc	L	u'
A	100	0.7	const.	const.
B	100	0.7	$\propto t^{0.5}$	$\propto t^{-0.5}$
C	191	0.7	$\propto t^{0.3}$	$\propto t^{-0.7}$
D	100	0.7	$\propto t^{0.7}$	$\propto t^{-0.7}$

[a] $Re_L = u'L/\nu$, where ν is the kinematic viscosity; Sc is the Schmidt number.

The LEM is implemented on a numerical grid which allows approximately six grid points per Kolmogorov length scale at the Reynolds numbers considered. The domain is periodic and fast Fourier transforms are used to compute the spatial derivatives. Since it has no source term in the current application, Fick's law has an exact solution in Fourier space, and the time step is controlled by the frequency of inversion events. Unless otherwise noted, the initial plume is represented by a discretized Gaussian profile which is the exact solution to the diffusion equation at $t/t_L = 0.01$ using a Dirac delta function as the initial condition, where $t_L = (L/u')|_{t=0}$ is the initial large eddy turnover time. In comparison with an initial condition of a plume one cell wide, the narrow Gaussian initial condition significantly reduces Gibb's phenomenon and the resulting unphysical negative scalar concentrations. We note that we first observed the LEM characteristics discussed here in simulations which implemented the diffusion mechanism using a finite difference method. The spectral technique yields equivalent results and requires less computational time to attain the same accuracy.

Simulation and experimental results for $(\theta'/\bar{\theta})_{CL}$ are exhibited in Fig. 1, where time is scaled by t_L. We see that the LEM not only predicts qualitatively the expected early time behavior, as previously noted by Kerstein [12], it also predicts a nonzero asymptote for the case of turbulence decaying with $u' \propto t^{1/2}$, i.e., the case where similarity is possible. Understood from the viewpoint of the model mechanisms, if the mapping length is greater than the plume width, an inversion is capable of displacing the entire plume and thus the plume can flap. This criteria is met only in cases B and D, assuming $d\sigma^2/dt \propto D_T$ at late time in grid turbulence. In case A the mapping length does not grow and a zero asymptote for $(\theta'/\bar{\theta})_{CL}$ is suggested, and in case C the mapping length grows but not fast enough to prevent a zero asymptote. A review of the results for case B in digital form shows $(\theta'/\bar{\theta})_{CL} = 0.21 \pm 0.03$

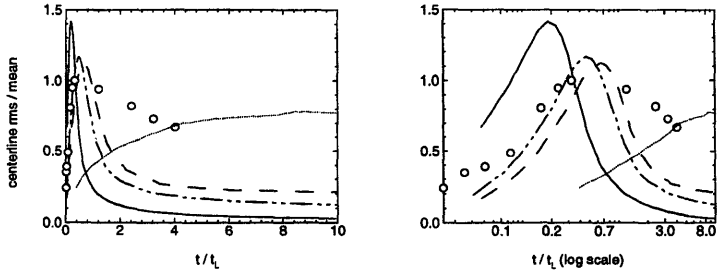

Fig. 1. Ratio of the rms temperature fluctuation to mean temperature along the centerline versus scaled time. Circles denote measurements [10]. Curves are predictions after 10,000 realizations for case A (solid), case B (dash), case C (dash-dot-dot), and case D (dotted).

from $t/t_L = 8.5$ to $t/t_L = 20$, exactly the behavior predicted by similarity analysis.

The asymptotic behavior of case D cannot be determined because it is impractical to advance the solution far enough in time at sufficient resolution to produce reliable results. However, it is included because it shows the dramatic effect on the results of the LEM of a small change in the turbulent decay rate. Both cases A and D show at best very qualitative agreement with the experimental data. When the decay mechanism is modeled more accurately as in cases B and C, the predictions of the LEM are quantitatively correct for $t/t_L < 1$, and exhibit the correct qualitative trends at a later time.

The finite asymptote of $(\theta'/\bar{\theta})_{CL}$ in case B suggests the self-similar behavior that is anticipated for turbulence decaying with $u' \propto t^{-1/2}$. Figure 2 shows the profiles for $\bar{\theta}$ at $t/t_L = 5.0$, 7.5, and 10.0 plotted in similarity form. It is seen that the profiles collapse to nearly the same curve when the ordinate is scaled by $t^{-1/2}$ and the abscissa is scaled by $t^{1/2}$. The figure also shows that the profiles of θ' collapse when scaled in the same manner. Therefore, for the decay scenario for which a self-similar solution is possible, LEM predicts self-similar behavior, further evidence that the model captures important aspects of the turbulent transport process.

Evaluation of the capability of the LEM in predicting the location of the plume requires a definition of the plume center. One measure is the first central moment of the scalar profile, y_c, i.e., the average of the distance of each

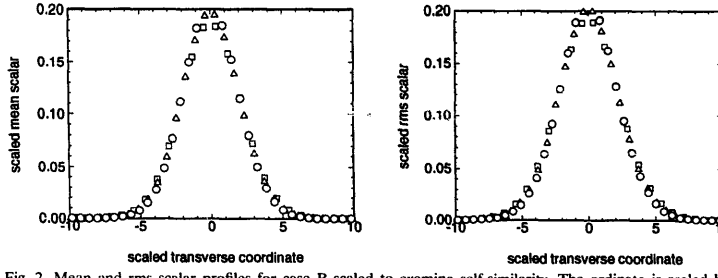

Fig. 2. Mean and rms scalar profiles for case B scaled to examine self-similarity. The ordinate is scaled by $t^{-1/2}$ and the abscissa is scaled by $t^{1/2}$. $t/t_L = 5.0$ (open square), 7.5 (open triangle), 10.0 (open circle).

point in the domain from some reference location weighted by the scalar concentration at that point. Mathematically,

$$y_c(t) \equiv \int_{-\infty}^{\infty} y\theta(y,t)\,dy.$$

By computing y_c at each time and at each realization, we can determine the probability density of y_c, $P(y_c)$. As predicted by random walk analysis, $P(y_c)$ is nearly Gaussian, except far from the centerline where the statistics are poor. Figure 3 shows $P(y_c)$ scaled so that a Gaussian plots as a straight line. The variance of y_c, σ^2, measures the range over which we can expect to find the center of the plume, and so is an indication of the tendency of the plume to wander. Of interest is how σ^2 evolves in time. Results for σ^2 are displayed in Fig. 4. In all cases at early times, σ^2 grows at approximately the rate predicted by random walk analysis, i.e., $\sigma^2 \propto t$. As time advances, σ^2 increases but at a decreasing rate; the range over which the plume wanders at late times becomes constant for case A and increases less rapidly for case B and especially for case C.

To see why the LEM predicts that σ^2 becomes constant for case A, we examine simulation results for nondecaying turbulence at very high Peclet number Pe. The results are exhibited in Fig. 5. In the first case, Pe $= \infty$ ($D_M = 0$) and the point source is represented by a finite value in a single numerical cell. This case simulates the dispersion of a fluid particle. In the second case, Pe = 100,000 with the same field initialization, so that the plume also spreads due to molecular diffusion. In the third and fourth cases, Pe $= \infty$ but the initial condition has the same amount of scalar distributed over 10 cells and 100 cells representing initial plume widths of $L/100$ and $L/10$, respectively. Of interest is the evolution of y_c.

For the first case, the plume behaves as predicted by random walk analysis. In the limit as Pe $\to \infty$, no molecular diffusion occurs and, since the plume is only one numerical cell wide and cannot be split by the inversion events, no growth of the plume itself due to inversion events can occur. The plume merely flaps back and forth. An ensemble average of 1000 realizations of this case shows a Gaussian profile

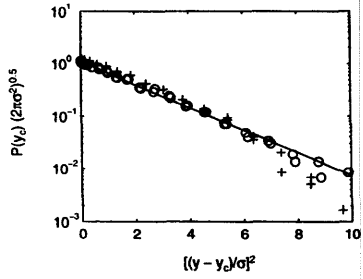

Fig. 3. The probability density of the plume center location scaled such that a Gaussian will plot as a straight line. The solid line denotes an exact Gaussian. The symbols represent behavior for case C at $t/t_L = 1$ (plus) and 10 (open circle). The observed Gaussian behavior over a large range of y is typical of all the simulations.

for the mean scalar centered at $y = 0$ at all times. The variance of y_c grows with t as expected for the statistically stationary case.

In the second case, all simulation parameters are the same as in the first case, except molecular diffusion is enabled, thereby reducing Pe to 10^6. We expect the first and second cases to be similar, i.e., the behavior at large Pe should go over to the behavior at infinite Pe. However, in the diffusive case, the plume ceases to flap before it has time to deviate far from the centerline. This behavior is not expected from physical arguments.

The mechanistic difference between the two simulations is that, in the nondiffusive case, the plume cannot be split but in the diffusive case it can be. Splitting the plume has the same effect as following multiple plumes, and hence the results are similar to those for multiple realizations of the nondiffusive case. The third and fourth cases emphasize this point. With no molecular diffusion but a plume width greater than one cell, the convective mappings fragment the plume and the results are similar to those for the diffusive case.

The case of very high Schmidt number and finite Reynolds number is addressed in order to isolate the cause of the inability of the model to accurately predict certain statistics at later times. In the formulation of the LEM, it is assumed that an ensemble average of model realizations at a given time step can be substi-

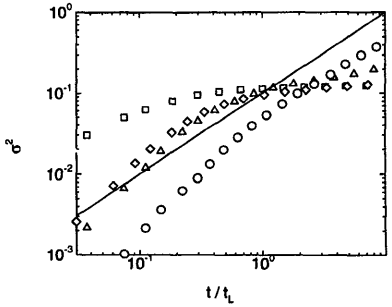

Fig. 4. The variance of the probability density of the plume center location versus scaled time. The solid line denotes expected behavior from random walk analysis. Symbols are predictions after 10,000 realizations for case A (open square), case B (open triangle), case C (open diamond), and case D (open circle).

tuted for a temporal average at a given downstream location in the laboratory, consistent with previous results noted by Kerstein [12]. The current results show that a single realization is in fact an average itself.

Further evidence of this can be seen by examining the width of the scalar profile for a single realization and comparing it to the width of the mean scalar profile. Due to the tendency of the plume to fragment, the individual profile is not continuous in y. Therefore plume width estimates based on the range of y over which the scalar concentration is greater than a given value are difficult to interpret. Instead we use the second central moment of the scalar profile. Figure 6 shows this moment for three realizations of case B along with the same moment computed from the mean profile after 10,000 realizations. We see that the profile width in each realization is about equal to the mean profile width.

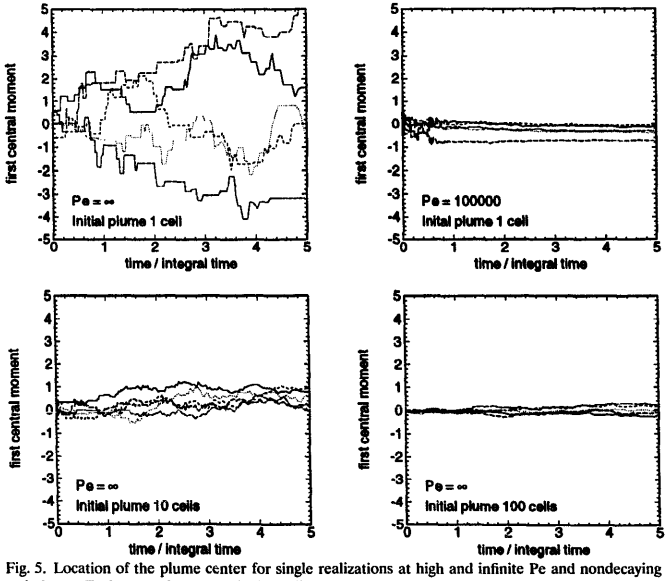

Fig. 5. Location of the plume center for single realizations at high and infinite Pe and nondecaying turbulence. Each curve denotes a single realization.

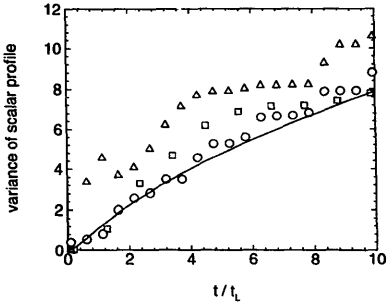

Fig. 6. Second central moment of the scalar profile for case B versus scaled time. The solid line represents the mean profile (10,000 realizations). The symbols represent profiles of individual realizations.

In the laboratory, the instantaneous plume width downstream from a heated wire does not include the effects of flapping, and hence is expected, especially at early times, to be significantly smaller than the mean plume width, which does include this effect. The time period over which this phenomenon should occur, however, has never been established either through theory or laboratory experiments. It is common to define three regimes of plume development: molecular–diffusive ($t \ll D_M/v'^2$), turbulent–convective ($D_M/v'^2 \ll t \ll t_L$), and turbulent–diffusive ($t \gg t_L$) (see, e.g., [9, 10]). Within this context, the initially smooth plume is moved about bodily by the turbulence and, at the same time, internal structure develops. This behavior characterizes the turbulent-convective regime. In the turbulent–diffusive regime, the plume has presumably grown to the size of the turbulent integral scale L, a patchy structure is well established, and the plume grows more by diffusion due to the smaller-scale turbulence than by flapping. These qualitative arguments are based upon experiments at moderate Reynolds numbers with Sc $\approx$ 1. However, it must be realized that the individual plume width can be made arbitrarily small by reducing D_M while holding Pe constant (that is, by increasing the Reynolds number), and so the ratio of the individual plume width to the mean plume width should not be linked to t_L, which is a property of the velocity field only.

In the simulations, the width of the individual plume is comparable to the mean plume width at all times, and, therefore, does not include flapping. A consequence of this can be seen in Kerstein's Fig. 3, which shows the turbulent–convective regime in the simulations to be unexpectedly short [12]. Examination of individual profiles reveals that the plume tends to fragment very early, often as a result of the first inversion event to affect the region of the domain containing the plume. This rather unphysical characteristic must be kept in mind when applying the LEM. It may be that it leads to erroneous predictions of some quantities that depend on the large-scale behavior of individual plumes. On the other hand, the model may perform very well in predicting the behavior of small-scale processes, e.g., differential diffusion. Thus, as is true for any model of turbulence, the usefulness of the model depends on the problem addressed. In addition, the fact that the plume is quickly split into many separate subplumes may make the model very practical for computing statistics not affected by this behavior, because very few realizations are required to produce a statistically steady ensemble. For further discussion of this latter point, see [1, p. 368].

4. CONCLUSION

When implemented with an appropriate turbulence decay scheme, the LEM predicts asymptotic behavior for $(\theta'/\bar{\theta})_{CL}$ consistent with similarity theory and experiments. The model also exhibits self-similar behavior for $\bar{\theta}$ and θ' expected from similarity theory. Furthermore, provided that the mapping length of the convective mappings increases at least as fast as the width of the plume increases, inversion events are capable of displacing the entire plume and the model reproduces the flapping motion of the physical plume.

Despite the improved performance of the LEM when turbulence decay is introduced, it is still unable to correctly predict the advection of a plume by the turbulence. The LEM tears the plume apart at early time causing each realization to evolve into multiple independent

plumes, and thus all the realizations are statistically equivalent at late time. This behavior must be considered when using the LEM to predict certain statistics.

We thank Dr. George Kosály, Dr. Alan Kerstein, and Dr. Donald Slinn for helpful discussions. This research was supported, in part, by National Science Foundation Grant No. CTS9415280.

REFERENCES

1. Kerstein, A. R., *J. Fluid Mech.* 231:361 (1991).
2. Kerstein, A. R., *J. Fluid Mech.* 216:411 (1990).
3. McMurtry, P. A., Menon, S., and Kerstein, A. R., *Twenty-Fourth Symposium (International) on Combustion*, The Combustion Institute, Pittsburgh, 1992, p. 271.
4. Menon, S., McMurtry, P. A., and Kerstein, A. R., in *Large Eddy Simulation of Complex Engineering and Geophysical Flows* (B. Galperin and S. A. Orszag, Eds.), Cambridge University Press, Cambridge, UK, 1993, p. 271.
5. Anand, M. S., and Pope, S. B., in *Turbulent Shear Flows 4: Selected Papers from The Fourth International Symposium on Turbulent Shear Flows, University of Karlsruhe, Karlsruhe, FRG, September 12-14, 1983* (L. J. S. Bradbury, F. Durst, B. E. Launder, F. W. Schmidt, J. H. Whitelaw, Eds), Springer-Verlag, New York, NY, 1985, p. 46.
6. Gifford, F., *Adv. Geophys.* 6:117 (1959).
7. Corrsin, S., *Méchanique de la Turbulence (Coll. Intern. du CNRS á Marseille)*, Presses du CNRS, Paris, 1962, p. 27.
8. Shlien, D. J., and Corrsin, S., *J. Fluid Mech.* 62:255 (1974).
9. Stapountzis, H., Sawford, B. L., Hunt, J. C. R., and Britter, R. E., *J. Fluid Mech.* 165:401 (1986).
10. Warhaft, Z., *J. Fluid Mech.* 104:363 (1984)
11. Tennekes, H., and Lumley, J. L., *A First Course in Turbulence*, MIT Press, Cambridge, MA, 1972.
12. Kerstein, A. R., *Combust. Sci. Technol.* 60:391 (1988).
13. Chandrasekhar, S., *Rev. Mod. Phys.* 15:1 (1943).

Received 16 September 1996; accepted 21 February 1997